

Numerical Investigation on Optimizing Fatigue Life in a Lap Joint Structure

P. Zamani, S. Mohajerzadeh, R. Masoudinejad, Kh. Farhangdoost

Abstract—Riveting process is one of the important ways to keep fastening the lap joints in aircraft structures. Failure of aircraft lap joints directly depends on the stress field in the joint. An important application of riveting process is in the construction of aircraft fuselage structures. In this paper, a 3D finite element method is carried out in order to optimize residual stress field in a riveted lap joint and also to estimate its fatigue life. In continue, a number of experiments are designed and analyzed using design of experiments (DOE). Then, Taguchi method is used to select an optimized case between different levels of each factor. Besides that, the factor which affects the most on residual stress field is investigated. Such optimized case provides the maximum residual stress field. Fatigue life of the optimized joint is estimated by Paris-Erdogan law. Stress intensity factors (SIFs) are calculated using both finite element analysis and experimental formula. In addition, the effect of residual stress field, geometry and secondary bending are considered in SIF calculation. A good agreement is found between results of such methods. Comparison between optimized fatigue life and fatigue life of other joints has shown an improvement in the joint's life.

Keywords—Fatigue life, Residual stress, Riveting process, Stress intensity factor, Taguchi method.

I. INTRODUCTION

AIRCRAFT fuselages are complex structures that are composed by many subassemblies together. Riveting is considered as an appropriate method for connecting elements of an aircraft fuselage. Lap joint is one of the most important ways of connecting the sheet metal parts. Riveted or bolted aircraft structures can be manufactured by either single or double lap joint. Failure in riveted joints can be catastrophic in aircraft industry. For example, the 1988 Aloha Airlines Flight 243 disaster, in which a portion of the passenger compartment disintegrated and resulted in one civilian casualty and several passengers sustained life threatening injuries, was attributed to a failure at and around one of the rivet holes, which propagated to the whole assembly [1]. Failure in riveted joints is affected by three main factors: stresses that are produced during riveting process, thermal fatigue, and vibration. Of these parameters, thermal fatigue and vibration are difficult to control [1]. So, controlling the stress field which is produced during the riveting process is very important. There are many factors that affect the joint's stress field such as riveting

squeeze force, clearance fit, friction coefficient, and sheet thickness.

An experimental study showed that increasing the riveting squeeze force results in increasing the residual stresses. Thus, the increase in squeeze force, improves fatigue life of the riveted joint [2]. Frost et al. [3] concluded that increasing the number of rows of rivet increases the fatigue strength of the joint, they also found the optimum spacing and position for the rivets array. Trego [4] investigated the effect of compression residual stresses besides the rivet hole which showed that greater compression residual stress can improve fatigue life of the joint. Rans [5] developed a simple finite element model in order to achieve residual stresses during the riveting process. Iyer et al. [6] developed a numerical procedure based on finite element modeling. The effect of countersinking the rivet head, its material, and friction between sheets are examined. They concluded that all these factors were increased with severity of the countersink. Muller [2] studied the effect of squeeze force on the fatigue life of rivet using finite element method for the first time. His study showed that using high squeeze force in riveting process could have a positive effect on fatigue life. Zhang et al. [7] presented mathematical and mechanical models for elastic, plastic and springback deformation of the rivet.

In general, the presence of holes, rivet contact, residual stress, and geometric discontinuity means that the riveted joints play a key role in assessing the structural integrity of an aircraft fuselage. Urban [8] provided an extensive summary of these works and carried out static and fatigue tests on different riveted joint configurations. Urban also showed that in order to obtain an accurate stress field with a view to establishing a good numerical/experimental correlation, a detailed finite element (FE) model is required. The papers written by Fung and Smart [9], [10] provided evidence of a numerical parametric and fatigue study of riveted lap joints. Using both numerical and experimental methods, they investigated the effect of clearance fit and friction and clamping force on the fatigue life of the joint. Their results confirm the effect of these parameters on the fatigue behavior of riveted sheet joints. Deng and Hutchinson [11] carried out an extensive FE analysis on simplified solid-rivet geometry in order to obtain the residual and clamping stresses. Szolwinski and Farris [12] analyzed the squeeze force effect on residual stress using a nonlinear 2-D FE model. These residual stresses are generally compressive near the rivet/hole interface and are tensile at the internal points far from the hole area. Moreira et al. [13] analytically and numerically evaluated the residual stress intensity factor (SIF) for different crack dimensions and for

P. Zamani, Ph.D. student, is with the school of Mechanical Engineering, Ferdowsi University of Mashhad, Mashhad, Iran (corresponding author to provide phone: +98-9112781293; e-mail: p.zamani@stu.um.ac.ir).

S. Mohajerzadeh, MSc student, R. Masoudinejad, Ph.D. student, and Kh. Farhangdoost, Associate Professor, are with the school of Mechanical Engineering, Ferdowsi University of Mashhad, Mashhad, Iran (e-mail: S.Mohajerzadeh@gmail.com, Masoudinejad@stu.um.ac.ir, farhang@um.ac.ir).

different value interferences. In any event, this interference is coupled with the squeeze force and, consequently, with the deformed rivet head dimensions.

The residual stress field is produced due to riveting process and hence the remaining residual stresses may have positive or negative effect on static and fatigue failure. Thus, it is important to check the effect of different factors on such stress field. This paper presents a study to determine the effect of variations in riveting process parameters, such as riveting squeeze force, clearance fit, friction coefficient and sheet thickness on the quality of stress field after riveting process. So, four levels are considered for each factor and an optimum joint is achieved using design of experiments (DOE) and Taguchi method. Then effect of parameters on residual stress field is estimated using analysis of variance (ANOVA). In continue, a crack is considered for the optimized joint that emanates from the sheet's hole. After that, fatigue life of the joint is calculated by considering the effect of geometry, secondary bending and residual stress.

II. FINITE ELEMENT MODELING

Because of the symmetry of the joint, only one half of the joint (Fig. 1) was modeled. Symmetric boundary conditions were applied to the joint center plane along the longitudinal direction. As shown in Fig. 1, boundary conditions of the joint during riveting process is defined as: displacement of the sheet's remote edges in y and z direction is zero, rivet head is restrained in y direction in order not to move during riveting process, symmetry in z direction is defined as mentioned before.

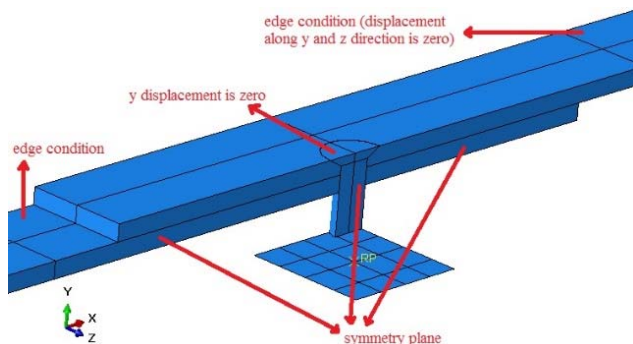


Fig. 1 Boundary conditions for simulating riveting process

TABLE I
MATERIAL PROPERTIES

Mode #	Young's Modulus (GPa)	Poisson ratio	Yield strength (MPa)	Hardening parameter	Paris power and coefficient
Rivet (2117-T4)	71.7	0.33	350	K=600, n=0.3	C=1.1e-7, m=3.6
Sheets (2024-T4)	72.4	0.33	368	K=500, n=0.3	C=4.7e-7, m=3.7

The material of the rivet and sheet is isotropic plasticity model with rate effects, which uses power hardening rule, with the following equation, $\sigma = K\varepsilon^n$, where σ is true stress, ε is true strain, K is the strength hardening coefficient and n is the

strength hardening exponent. The material properties used in the simulations are from Rijck et al. (2007) as shown in Table I [14].

Contact condition is defined between surfaces as: connection between hammer and rivet, connection between rivet and sheets (rivet and lower sheet, rivet and surface of the hole) and connection between two sheets. The connection is defined as explicit surface to surface contact. The solution type is defined as Dynamic/Explicit because of large deformations during riveting process. A constant force is applied to the rigid body in order to deform the rivet's leg and form the riveted joint (loading phase). Then, the force is defined as zero in the second step (unloading phase) and the rigid body has moved back. Eight node standard 3D axisymmetric elements are chosen in modeling the joint. Besides that, reduced integration is also applied. Riveting process contains large plastic deformation of the rivet. So, the elements will be distorted because of such large deformation. Element distortion increases computational time and also can stop simulation. Adaptive meshing is used to minimize distortion of elements. Distortion control option is also activated. A typical mesh of axisymmetric model is shown in Fig. 2.

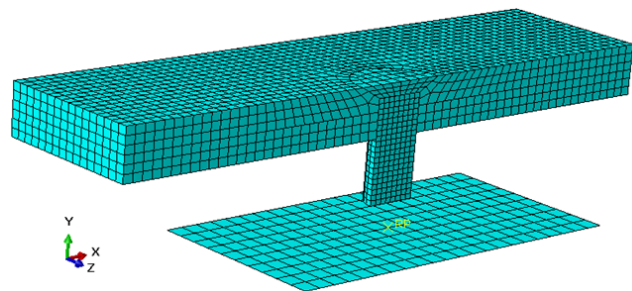


Fig. 2 The meshed model of simple riveted lap joint

III. OPTIMIZATION OF THE JOINT

In order to understand and analyze the effect of variations in the riveting process parameters on residual stress field, a design of experiment (DOE) is first carried out based on Taguchi's orthogonal array. Also it is known that higher residual stress field improves fatigue life of the joint. So, effect of parameters on residual stress field is evaluated. Then, optimized parameters and their optimum levels are calculated using Taguchi method. Also, effect of each parameter on residual stress field is estimated using analysis of variance (ANOVA). Finally, fatigue life of the single lap joint is computed using Paris-Erdogan law by considering the effect of geometry, secondary bending and residual stress. It should be noted that Taguchi method provides two main results: (1) shows which level of each parameter causes maximum residual stress, (2) it also shows the parameter that has the most effect on residual stress changes among other parameters.

Friction coefficient, clearance fit, riveting squeeze force and sheet thickness is four factors that are considered in this study.

The four factors under study are considered at four levels, as discussed later. It takes lots of cost and time to study the effect of multi-level factors in a system because it is necessary to consider all possible cases for experimenting. However, Taguchi has presented his tables in order to optimize the number of experiments. Taguchi's L_{16} orthogonal table is used for designing experiments in this paper (relates to four factors that each factor has four levels). This table decreases 256 possible experiments to 16 experiments. Four factors with their corresponding levels are shown in Table II. Design of experiments for this study is also shown in Table III.

TABLE II
EFFECTIVE PARAMETERS AND THEIR LEVELS

Factor	Friction coefficient	Clearance fit	Riveting squeeze force	Sheet thickness
Level 1	0.2	0	7	2
Level 2	0.4	0.05	10	2.2
Level 3	0.6	0.1	13	2.4
Level 4	0.8	0.2	16	2.6

TABLE III
TAGUCHI DESIGN OF EXPERIMENTS

Number of experiment	Friction coefficient	Clearance fit	Riveting squeeze force	Sheet thickness
1	0.2	0	7	2
2	0.2	0.05	10	2.2
3	0.2	0.1	13	2.4
4	0.2	0.2	16	2.6
5	0.4	0	10	2.4
6	0.4	0.05	7	2.6
7	0.4	0.1	16	2
8	0.4	0.2	13	2.2
9	0.6	0	13	2.6
10	0.6	0.05	16	2.4
11	0.6	0.1	7	2.2
12	0.6	0.2	10	2
13	0.8	0	16	2.2
14	0.8	0.05	13	2
15	0.8	0.1	13	2.6
16	0.8	0.2	7	2.4

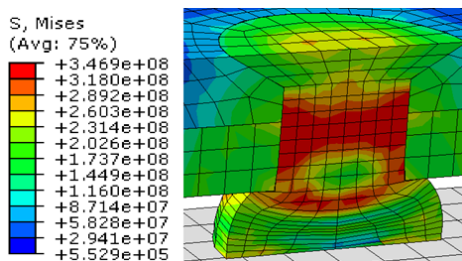


Fig. 3 Residual stress field (10th experiment)

Finite element modeling is accomplished for each experiment in Table IV and the results of maximum residual stress are stated in Table IV. Residual stress state in the 10th experiment is shown in Fig. 3. In continue, loss function is defined in a higher-better condition, because the higher residual stress field results in better fatigue life. In other

words, higher-better condition belongs to the situation in which higher amount of goal function is appropriate.

Loss function is defined as:

$$L = \frac{1}{n} \sum \left(\frac{1}{y_i} \right)^2 \tag{1}$$

where n is the try number for each experiment, i is the number of experiment, and y is the maximum residual stress (goal function). Then, signal to noise ratio is calculated as:

$$SN = -10 \log(L_i) \tag{2}$$

where L is the loss function and i is the number of experiment. So, the amount of loss function and signal to noise ratio are calculated for each experiment and are shown in Table IV. In continue, mean of signal to noise ratio for each factor is calculated for each level. For example, mean of SN ratios are calculated for the first factor (Riveting squeeze force) and in its first level. This calculation relates to mean of signal to noise ratio for the first level of riveting squeeze force. Mean of SN ratio for other factors and their corresponding levels are calculated using such method (Table V). Δ in Table V is defined as the difference between maximum and minimum amounts of mean SN ratio for each factor among its different levels. The factor that has the maximum amount of Δ , has the most effect among other factors on the residual stress field. The most and least amount of Δ are belong to riveting squeeze force and clearance fit, respectively. It means that variations in riveting squeeze force affect the most on residual stress field in compare with the same variation in other factors. Priority of factors is introduced as rank numbers in Table V. Variations in the lower rank number has more effect on residual stress field.

TABLE IV
MAXIMUM RESIDUAL STRESS, LOSS FUNCTION AND SIGNAL TO NOISE RATIO FOR EACH EXPERIMENT

Number of experiment	Maximum residual stress (MPa)	Loss function	Signal to noise ratio (SN)
1	341.4	8.5797	50.6653
2	348	8.2574	50.8316
3	344.8	8.4113	50.7514
4	343.9	8.4554	50.7287
5	342.3	8.5347	50.6881
6	333.8	8.9749	50.4697
7	349.6	8.1820	50.8714
8	347.4	8.2859	50.8166
9	348.1	8.2526	50.8341
10	346.9	8.3435	50.7865
11	342.5	8.5247	50.6932
12	348	8.2574	50.8316
13	347.4	8.2859	50.8166
14	344	8.4505	50.7412
15	343.3	8.4850	50.7135
16	340.5	8.6251	50.6424

TABLE V
MEAN OF SIGNAL TO NOISE RATIO AND RANK NUMBER FOR EACH FACTOR

Factor	Friction coefficient	Clearance fit	Riveting squeeze force	Sheet thickness
Level 1	50.7443	50.7510	50.6176	50.7774
Level 2	50.7114	50.7073	50.7662	50.7895
Level 3	50.7863	50.7574	50.7858	50.7171
Level 4	50.7284	50.7726	50.8008	50.6865
Δ	0.0749	0.0653	0.1832	0.1030
Rank	3	4	1	2

Means of SN ratio are shown in Fig. 4 for each factor and according to different levels. As it is shown in Fig. 4, maximum amount of Δ belongs to riveting squeeze force. However, maximum amount of Mean SN ratio could be understand for each factor in different levels (Fig. 4). Maximum amount of mean for riveting squeeze force is happened in its last level according to Fig. 4. The maximum means of SN ratio for friction coefficient, clearance fit and sheet thickness are in their third, fourth and second levels, respectively. The mentioned levels are defined as optimum levels which can be used in design and fatigue analysis and maximize the residual stress field. In order to verify the optimum factors (optimum joint), a 3D simulation of riveting process is conducted due to optimum levels of each factor. Then, result of this simulation is derived and corresponding SN ratio is calculated. In continue the error between the optimum SN ratio and other SN ratios is computed. The comparison has shown a mean error of 4.82% between SN ratio for optimum joint and other experiments. So, effects of friction coefficient, fastener clearance fit, hammer squeeze force and thickness of the sheet is studied numerically on the stress state in a simple riveted lap joint.

IV. FATIGUE LIFE CALCULATION

Fatigue cracks are characterized as non-propagating cracks before ΔK_{th} . Microstructure, mean stress, frequency, and environment mainly control region I crack growth. Region II shows essentially a linear relationship between $\log da/dN$ and $\log \Delta K$ [15]. This linear relationship corresponds to the formula suggested by Paris and Erdogan [16]:

$$\frac{da}{dN} = C(\Delta K)^m \quad (3)$$

where m and C are power and coefficient of Paris-Erdogan relationship, respectively. Thus, fatigue life can be calculated by integrating (3). So, the most important part in computation of fatigue life is calculating accurate amounts of stress intensity factors. SIF calculation can be performed in two ways: (1) calculation of SIF by considering experimental and theoretical formulas for emanating crack from hole. Experimental formula considers the effect of geometry and residual stress field and theoretical equation calculates SIFs corresponding to secondary bending effect, (2) calculation of SIF through finite element analysis. Three main stages of the first method are as follows:

- Calculation of stress intensity factors corresponding to geometry of crack
- Calculation of stress intensity factors corresponding to residual stress effect around the rivet hole
- Calculation of stress intensity factors corresponding to secondary bending effect

Then, fatigue life is calculated using the total stress intensity factor. Such total stress intensity factor is considered the effect of residual stress and secondary bending through experimental and theoretical formulas. In continue, a finite element analysis is carried out using ABAQUS 6.11 to calculate SIFs. Finally, fatigue life of the riveted joint is estimated using both methods.

A. First Method in SIF Calculation

Schijve et al. carried out a couple of experimental tests and presented an experimental correction coefficient for stress intensity factor. Correction coefficient is defined in (4). So K_I can be calculated through $K_I = \beta \sqrt{\pi a}$.

$$\beta = \left[\frac{I}{0.539 + 1.93 \frac{a}{R} + 2 \left(\frac{a}{R} \right)^2} + \frac{\lambda + 2}{2} \right] \sqrt{\frac{\lambda + I}{2} \left[I + \frac{a}{R} \frac{\lambda^3}{5} \right]} \quad (4)$$

where a and R are crack length and hole radius, respectively. λ is defined as:

$$\lambda = \frac{I}{1 + \frac{a}{R}} \quad (5)$$

Schijve's experimental formula is based on Newman's experimental results. He also considered the effect of width, hole effect, and crack length in such formula. Equation (4) considers the effect of loading and geometry in calculation of stress intensity factor. There are other important factors that affect the amount of stress intensity factor: the effect of residual stress on SIF and the effect of secondary bending.

Beuth and Hutchinson presented a relationship for cracks emerging from a rivet hole where there is a pre-existing residual stress field due to the riveting process (6) [17].

$$\frac{K}{\sigma_R \sqrt{R}} = \sqrt{\pi \frac{a}{R}} G \left(\frac{a}{R} \right) \quad (6)$$

where a , R , σ_R and $G \left(\frac{a}{R} \right)$ are crack length, radius of hole, maximum residual stress and a function that is defined by Beuth and Hutchinson. Beuth and Hutchinson stated that a reasonable estimate for σ_R should fall between half of the yield strength and yield strength of the sheet material [17]. Also, maximum residual stress is achieved as 185 MPa after simulating riveting process.

Secondary bending is one of the most important factors that effect on stress intensity factor. Calculation of secondary bending stresses is based on advanced beams theory. Rijck et al. used neutral line model to calculate stresses in a simple lap

joint due to secondary bending effect. They finally presented (7) as secondary bending coefficient [18].

$$K_b = \frac{3}{1 + 2\sqrt{2} \tanh(\alpha L)} \tag{7}$$

where L is shown in Fig. 5 and α is defined as:

$$\alpha = \sqrt{\frac{3\sigma}{2t^2 E}} \tag{8}$$

σ , t and E stands for stress, sheet thickness and module of elasticity, respectively. Equation (7) implies that the effect of the length of specimen on the secondary bending can be ignored.

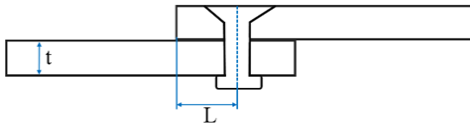


Fig. 5 Schematic of secondary bending parameters

Stress intensity factors are calculated by considering effect of geometry of crack, residual stress and secondary bending and dimensions are related to the optimized joint's dimensions. Table VI shows stress intensity factors due to each factor. Then, final stress intensity factor for each crack length is calculated by summing three SIFs.

TABLE VI
STRESS INTENSITY FACTORS CORRESPONDING TO GEOMETRY, RESIDUAL STRESS AND SECONDARY BENDING EFFECT FOR EACH CRACK LENGTH

Crack length (m)	0.5e-4	0.7e-4	1e-4	1.2e-4	1.5e-4	1.7e-4	2e-4
K_I	2.9769	3.2877	4.1064	4.3532	4.7033	5.0167	5.3579
K_R	3.2	3.36	3.51	3.69	3.85	3.97	4.09
K_b	3.5124	3.6823	3.6923	3.7113	3.8115	3.8391	3.8453
K_{total}	3.2893	3.61	4.2887	4.3745	4.6648	4.8858	5.1132

B. Second Method in SIF Calculation

Fatigue life calculation of the riveted joint can be carried out using either linear elastic fracture mechanics (LEFM) or Elastic-plastic fracture mechanics (EPFM). In LEFM, local stresses in the vicinity of crack tip are solved according to elasticity theory. So, study of crack and fatigue crack growth is accomplished through computation of SIFs. This approach is valid until the time that the plastic zone in the vicinity of crack (plastic radius) can be ignored in compare with the length of crack. In this paper, an emanating linear semi elliptical crack is considered for the optimized lap joint.

First of all, the riveting process is simulated with a 16 kN riveting force, 2.2 mm sheet thickness, friction coefficient of 0.6 and a 0.2 mm clearance fit (related to optimum joint). Then, an elliptical crack emanating from the sheet's hole is defined as it is shown in Fig. 6.

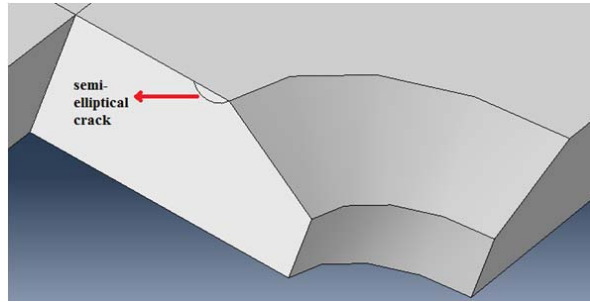


Fig. 6 Semi-elliptical crack emanating from sheet's hole

Solution step is defined as Dynamic/Explicit in finite element software. Loading condition is defined as cyclic tension load with constant amplitude. Direction of load is along the length of the sheet and it is applied to the two side of the sheets. Stress ratio (R) and frequency are considered as zero and 20 Hz, respectively. Maximum applied cyclic stress is 30 MPa. After simulating the riveting process and applying load conditions, stress intensity factors are calculated. These SIFs are computed for different crack lengths. Fig. 7 shows a comparison between Newman's SIFs and FEM results for different crack lengths.

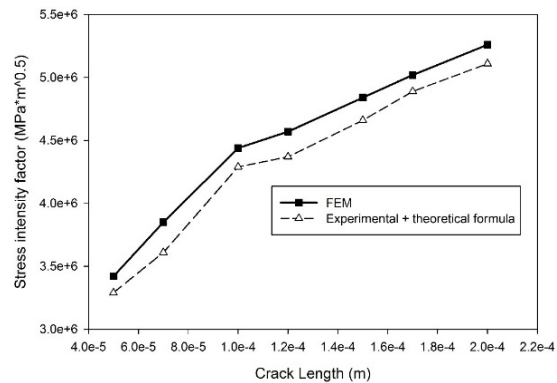


Fig. 7 Stress intensity factors resulted from FEM and experimental formula

Fig. 6 shows a mean error of 4% between FEM results and experimental formula. In continue, fatigue life of the riveted joint is calculated using Paris model. Fatigue life calculation is performed in each crack length. It should be noticed that fatigue life computation is based on two set of SIF results: FEM and formulation results. Fatigue life of such methods is shown in Fig. 8.

Another simulation process is accomplished for a number of experiments to achieve stress intensity factors. The crack geometry, loading and boundary conditions are the same as mentioned before. SIFs are calculated through finite element solution and fatigue life is estimated for all other experiments. As it is shown in Fig. 9, experiments number 2 and 6 has lower fatigue life than optimum fatigue life because maximum residual stress field belongs to optimum joint. In addition, fatigue life of the 4th experiment is higher than 2nd and 6th experiments because the levels of four factors in this

experiment are closer to optimum joint than the other two experiments.

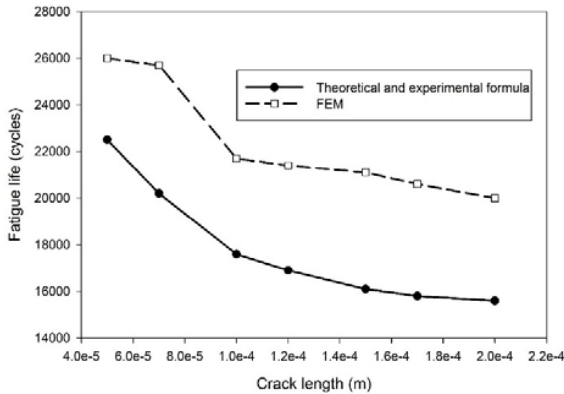


Fig. 8 Fatigue life variation for different crack length

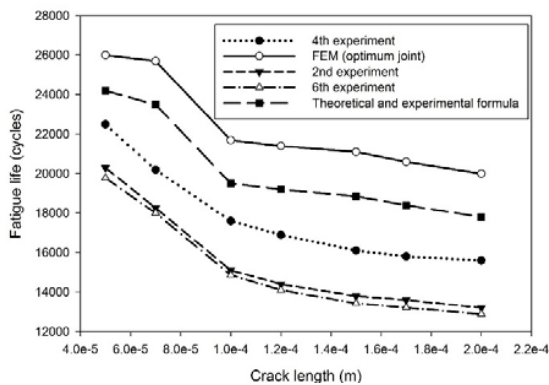


Fig. 9 A comparison between optimum fatigue life cycle and other experiments

V. CONCLUSION

A 3D finite element method simulation and analysis is carried out on a simple riveted lap joint in order to achieve residual stress field for each experiment in Taguchi's orthogonal array. A Taguchi method is used to determine the effect of four factors on the residual stress field in a simple riveted lap joint. Four levels are considered for each factor. Then, optimized factors are achieved to maximize the residual stress field. After accomplishing the Taguchi procedure and fatigue life estimations, following conclusions are drawn:

1. Residual stress field's sensitivity to variation is mostly dependent to riveting squeeze force and least dependent to clearance fit. In other words, a little change in riveting squeeze force causes much variation in residual stress field than the same change in other factors.
2. Optimum levels for riveting squeeze force, friction coefficient, clearance fit and sheet thickness are in their 4th, 3rd, 4th and 2nd levels, respectively.
3. The increase in riveting squeeze force improves residual stress field. Although, the increase in sheet thickness has negative effect on residual stress field.
4. When there are some restrictions in dimension and space in design, the knowledge about the most sensitive factor

can be very useful to increase the residual stress field. Besides that, levels of each factor in which the maximum amount of residual stress field occurs, are determined and the optimum levels for riveting squeeze force, friction coefficient, sheet thickness and clearance fit are achieved.

5. A comparison is conducted between SN ratio of optimum joint and SN ratio of other experiments. A 4.82% error is found from this comparison and shows the validity of the optimum case.
6. The optimum joint has a higher fatigue life than other experiments. So it can be inferred that the maximum fatigue life is occurred in the optimum joint because it is optimized and designed based on maximizing residual stress field. Also, the more the levels of the four parameters close to their optimum condition, the more increase in fatigue life can be achieved. Thus it can be concluded that optimum joint has the highest fatigue life among all other possible combinations in levels of the four factors and optimization procedure has increased fatigue life.
7. Fatigue life of the optimum joint is estimated through finite element and experimental formulations and good accordance is found between such methods.

REFERENCES

- [1] S.H. Cheraghi, Effect of variations in the riveting process on the quality of riveted joints. *Int J Adv Manuf Technol* 2008; 39: 1144-1155.
- [2] R.P.G. Muller. An experimental and analytical investigation on the fatigue behavior of fuselage riveted lap joints. PhD thesis, Delft University of Technology, Delft, The Netherlands: 1995.
- [3] N.E. Frost, K.J. Marsh, L.P. Pook, *Metal fatigue*. Oxford University Press, London, 1974.
- [4] A. Trego, D. Cope, Evaluation of damage tolerance analysis tools for lap joints. *AIAA Journal* 2001; 39(12): 2250-2254.
- [5] C. Ransé, P.V. Straznický, Riveting process induced residual stresses around solid rivets in mechanical joints. *Journal of Aircraft* 2007; 44(1): 323-329.
- [6] K. Iyer, C.A. Rubin, G.T. Hahn, Three-dimensional analysis of single rivet row lap joints-part I: Elastic-Plastic response. *Recent Adv Solids Struct* 1999; 398: 41-57.
- [7] Z. Kaifu, C. Hui, L. Yuan, Riveting process modeling and simulating for deformation analysis for aircraft's thin-walled sheet-metal parts. *Chinese Journal of Aeronautics* 2011; 24: 369-377.
- [8] M.R. Urban, Analysis of the fatigue life of riveted sheet metal helicopter airframe joints. *International Journal of Fatigue* 2003; 25: 1013-1026.
- [9] C.P. Fung, Smart J., Riveted single lap joints. Part 1: Fatigue life prediction. *Proceedings of the institution of mechanical engineers, part G (Journal of Aerospace Engineering)* 1997; 211(1): 13-27.
- [10] C.P. Fung, Smart J., Riveted single lap joints. Part 2: A numerical parametric study. *Proceedings of the institution of mechanical engineers, part G (Journal of Aerospace Engineering)* 1997; 211(2): 123-128.
- [11] X. Deng, J.W. Hutchinson, The clamping stress in a cold driven rivet. *International Journal of Mechanical Sciences* 1998; 40(7): 683-694.
- [12] M.P. Szolwinski, T.N. Farris, Linking riveting process parameters to the fatigue performance of riveted aircraft structures. *Journal of Aircraft* 2000; 37(1): 130-137.
- [13] P.M.G.P. Moreira, P.F.P. de Matos, S.T. Pinho, D. Pastrama, P.P. Camanho, P.M.S.T. de Castro, The residual stress intensity factors for cold-worked cracked holes: A technical note. *Fatigue and Fracture of Engineering Materials and Structures* 2004; 27(9): 879-886.
- [14] J.J.M. Rijck, J.J. Homan, J. Schijve, R. Benedictus, The driven rivet head dimensions as an indication of the fatigue performance of aircraft lap joints. *International Journal of Fatigue* 2007; 29: 2208-2218.
- [15] H.K. Yoon, S.P. Lee, B.H. Min, S.W. Kim, Y. Katoh, A. Kohyama. Fatigue life and fatigue crack propagation behavior of JLF-1 steel. *Fusion Engineering and Design* 2002; 61: 677-682.
- [16] P.C. Paris, F. Erdogan, A critical analysis of crack propagation laws. *Transactions ASME Journal of Basic Engineering* 1963; 85: 528-534.

- [17] J.L. Beuth, J.W. Hutchinson, Fracture analysis of multi-site cracking in fuselage lap joints, *Computational Mechanics* 1994:13: 315-331.
- [18] J.J.M. Rijck, S.A. Fawaz, Schijve J., Benedictus R., Homan J.J., Stress analyses of mechanically fastened joints in aircraft fuselages, 24th ICAF Symposium, Naples, 2007.